Lanthanide−Transition-Metal Complexes: From Ion Pairs to Extended Arrays

CHRISTINE E. PLEČNIK, SHENGMING LIU, AND SHELDON G. SHORE*

Department of Chemistry, The Ohio State University, Columbus, Ohio 43210

Chart 1

$(L)_x Ln \!\!-\!\! M(L')_y \qquad [Ln(solvent)_x]_m [M(L')_y]_n$

(A)   **(B)**

$(L)_x Ln \!\!-\!\! \boxed{L'} \!\!-\!\! M(L')_y$

(C)

Ln = Lanthanide metal
M = Transition metal
L, L' = Various ligand sets

$-\boxed{L'}-$ = Bridging ligand

ABSTRACT

New lanthanide−transition-metal (Ln−M) compounds were prepared and the structural relationships of the metal combinations were discerned. Numerous compounds derived from divalent or trivalent lanthanides and from transition metals in groups 7−11 were isolated. Three different types of interactions were observed: (1) Ln−M direct bonds, (2) ionic associations, and (3) carbonyl or cyanide linkers between the metals. These assorted Ln−M interactions influence the assembly of the compounds, and discrete molecules or polymeric arrays were encountered. The extended arrays spanning one, two, and three dimensions can function as heterogeneous catalyst precursors. Two classes of systems, Ln−M carbonyls and cyanides, are described.
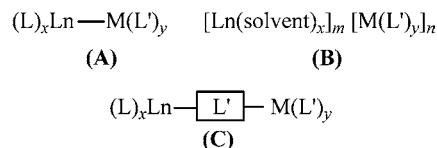
1. Introduction

The chemistry of Ln−M compounds dates back almost a century. The origin of one class can be traced to 1916, when a series of lanthanide hexacyanocobaltates, Ln[Co-(CN)$_6$]·nH$_2$O, were synthesized.[1a] Almost 60 years later, single-crystal X-ray diffraction analyses of these complexes revealed structures composed of infinite polymeric arrays that are supported by cyanide bridges, Ln−NC−M.[1b] In the 1970s, another group of compounds, Ln−M carbonyls, was being developed.[1c] Andersen and co-workers made great strides in the early 1980s toward understanding Ln−M interactions by determining the structures of several isocarbonyls, Ln−OC−M.[1d] Since these earliest contributions, numerous Ln−M compounds have been prepared.
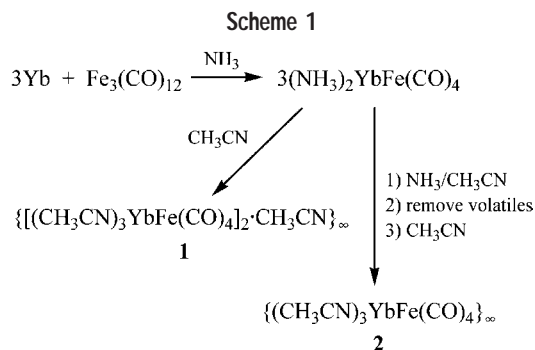
Research in this field has progressed for at least three reasons. First, the curiosity to develop new types of heterometallics has encouraged creative synthetic approaches. Second, the determination of the structural relationship between the two metals has revealed three different Ln−M complexes: (A) species with direct Ln−M bonds, (B) ionic systems, such as solvent-separated ion pairs, and (C) compounds with ligand bridges between the metals (Chart 1). Finally, the development of these mixed-metal compounds has led to their application in materials science and catalysis.[2]

We initiated our Ln−M studies in the early 1990s. At that time, several Ln−M carbonyl compounds were reported to have direct bonds on the basis of IR spectroscopic evidence.[3a] However, only one was confirmed by single-crystal X-ray diffraction to have a Ln−M bond.[3b] Therefore, the elusiveness of metal−metal bonded systems was our primary motivation for entering this area. We designed synthetic procedures that concentrated on the construction of bonds between Ln(II) species and transition metal carbonyl anions, [M(CO)$_y$]$^{n-}$. This endeavor led to the preparation of Yb−Fe bonded compounds that have extended arraylike structures framed by Yb−Fe bonds and Yb−OC−Fe isocarbonyl linkages. Since [M(CO)$_y$]$^{n-}$ anions have varying nucleophilicities, we were able to control the degree of interaction between Ln and M by simply changing [M(CO)$_y$]$^{n-}$. For instance, we developed syntheses for Ln−M carbonyl solvent-separated ion pairs by using weak nucleophilic [M(CO)$_y$]$^{n-}$ reagents.

The possibility of forming ligand-bridged systems and extended arrays steered us toward the study of Ln−M cyanide derivatives. Even though direct Ln−M bonds are not afforded, the bridging cyanide connections within the infinite polymers yield interesting structures. Some of the products are potentially useful as catalyst precursors and magnetic materials. For example, our cyanide compounds can be impregnated onto an oxide support without destroying the Ln−NC−M linkages. In fact, the structural framework is maintained, and the precursor complex can be converted to catalytic bimetallic nanoparticles.[4] Over the past few years, we have systematically synthesized and characterized a variety of Ln(II,III)−M(group10,group11) cyanide-bridged arrays. New types of extended networks that have various dimensionalities, including chains,

Christine E. Plečnik was born in Long Beach, CA, in 1974. She earned her chemistry B.S. degree from the University of California, Irvine. She joined the Shore Group soon afterward and has studied inorganic and organometallic systems. She was awarded graduate research industrial fellowships from Procter & Gamble and Lubrizol.

Shengming Liu was born in Hebei, China, and obtained his B.S. degree at Lanzhou University. He received his M.S. and Ph.D. degrees from Lanzhou Institute of Chemical Physics, Chinese Academy of Sciences. After a postdoctoral appointment in David A. Atwood's Group at the University of Kentucky, he joined the Shore Group. His research interests focus on synthesis, structural characterization, and application of new materials and catalysts.

Sheldon G. Shore was born in Chicago and received his B.S. degree from the University of Illinois. He obtained his M.S. and Ph.D. degrees from the University of Michigan. He joined the faculty at The Ohio State University and is a Distinguished Scholar, Distinguished Lecturer, and Charles H. Kimberly Chair of Chemistry. Some of his honors and recognitions include corresponding member of the Bavarian Academy of Science, Morley Award and Medal of the Cleveland Section of the American Chemical Society for Outstanding Contributions to Chemistry, Reilly Lecturer at the University of Notre Dame, and Wiberg Lecturer at the University of Munich, Germany. His research interests span main group, transition metal, and lanthanide chemistries, with applications directed toward materials science and catalysis.

* To whom correspondence should be addressed. E-mail: shore.1@osu.edu.

Scheme 1

$$3Yb + Fe_3(CO)_{12} \xrightarrow{NH_3} 3(NH_3)_2YbFe(CO)_4$$

CH₃CN ↓

$$\{[(CH_3CN)_3YbFe(CO)_4]_2 \cdot CH_3CN\}_\infty$$

1

1) NH₃/CH₃CN
2) remove volatiles
3) CH₃CN

$$\{(CH_3CN)_3YbFe(CO)_4\}_\infty$$

2

layers, columns, and anionic arrays with lanthanide cations sequestered in pockets, have been discovered.

2. Ln(II)−M Carbonyls

Before beginning work on Ln−M carbonyls, we proposed[5] that divalent lanthanide cations (Eu^{2+}, Sm^{2+}, Yb^{2+}) would have a greater chance of forming bonds with transition metals than harder Lewis acidic trivalent lanthanides. In a similar vein, we believed that soft Lewis basic and strongly nucleophilic transition metal carbonylate anions are beneficial for a direct Ln−M interaction. On the basis of these assumptions, three different synthetic approaches toward Ln(II)−M carbonyl complexes were employed: (1) reduction in liquid ammonia, (2) lanthanide/mercury amalgam reduction, and (3) transmetalation (metal exchange reaction). All three procedures utilize a lanthanide metal to reduce a transition metal carbonyl reactant.

The products from these reactions were found to be highly contingent upon the nucleophilicity of $[M(CO)_y]^{n-}$. The relative Lewis basicities of the transition metal center, the carbonyl ligands, and the coordinating solvent determine the degree of interaction between Ln and M. Three different types of products can form. Direct Ln−M bonded systems (structure A of Chart 1) are yielded when the transition metal center is the most nucleophilic constituent (i.e., the electron density resides on the transition metal). A solvent-separated ion pair (structure B of Chart 1) ensues when the electron donating ability of the solvent is stronger than $[M(CO)_y]^{n-}$. As a consequence, the solvent molecules occupy all of the available coordination sites on the lanthanide cation. An isocarbonyl, Ln−OC−M (structure C of Chart 1), is afforded when the carbonyl oxygen is more nucleophilic than the transition metal center. The result is the donation of an electron pair from a carbonyl oxygen to the lanthanide. Our results in this area are now summarized based on the bonding relationship of the Ln(II)−M carbonyls.

2.1. Metal−Metal Bonded Compounds. Very nucleophilic transition metal carbonylate anions are the preferred reagents for designing Ln−M bonded products (structure A of Chart 1). A prime candidate that has strong donating properties is $[Fe(CO)_4]^{2-}$. By linking this anion with Yb(II), we were one of the first to synthesize and structurally characterize (by single-crystal X-ray diffraction) Ln−M bonded systems.[5,6]

Reduction of $Fe_3(CO)_{12}$ with three equivalents of Yb metal in liquid ammonia produces $(NH_3)_2YbFe(CO)_4$

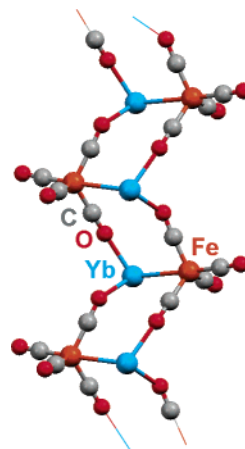**FIGURE 1.** 1-D polymeric ladder of $\{[(CH_3CN)_3YbFe(CO)_4]_2 \cdot CH_3CN\}_\infty$ (**1**).
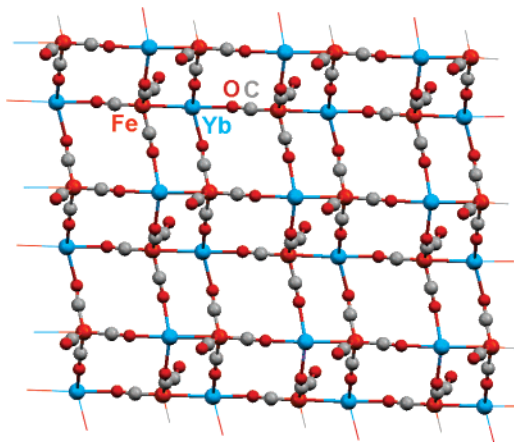
FIGURE 2. 2-D extended sheet of $\{(CH_3CN)_3YbFe(CO)_4\}_\infty$ (**2**).

(Scheme 1).[5,6] Dissolving $(NH_3)_2YbFe(CO)_4$ in CH₃CN causes the displacement of ammonia. Crystal structure analysis of the product, $\{[(CH_3CN)_3YbFe(CO)_4]_2 \cdot CH_3CN\}_\infty$ (**1**), reveals a 1-D polymeric ladder that is constructed by the combination of Yb−Fe interactions and isocarbonyl linkages (Figure 1).[7] Two carbonyls on each {Fe(CO)₄} unit participate in these isocarbonyl joints, which form ···Yb−OC−Fe−CO−Yb··· zigzag chains. Ytterbium−iron bonds couple the chains together, and they constitute the rungs of the ladder. In a slightly modified procedure, {(CH₃CN)₃YbFe(CO)₄}∞ (**2**) is isolated by quenching the $(NH_3)_2$-YbFe(CO)₄ reaction with CH₃CN, removing the volatiles, and redissolving the solid in CH₃CN (Scheme 1). Compound **2**'s structure is related to **1**'s, but additional carbonyl bridges between the ladders create a 2-D sheet (Figure 2; three carbonyls on each {Fe(CO)₄} moiety engage in isocarbonyl interactions). The most salient characteristics in the structures of **1** and **2** are the Yb−Fe bonds, which measure 3.010(1) and 3.046(1) Å, respectively. The bonds are comparable in length to those in $YbFe_2$ alloy (3.00 Å) and are shorter than the sum of the metallic radii (3.2 Å). An interesting facet of the production of **1** and **2** is that Yb initially reduces Fe to form $[Fe(CO)_4]^{2-}$, which then serves as a nucleophile to produce the Yb−Fe dative bond. The distribution of charge in the bond is problematic.[8]

Scheme 2

$$Yb/Hg \ + \ 2Fe(CO)_5 \xrightarrow[\text{-2CO}]{CH_3CN} \ [Yb(CH_3CN)_x] \, [Hg\{Fe(CO)_4\}_2]$$
$$\textbf{12}$$

DIME/CH₃CN ↙   ↓ Pyr/CH₃CN

$$[(DIME)_2Yb(CH_3CN)_2] \, [Hg\{Fe(CO)_4\}_2]$$
$$\textbf{13}$$

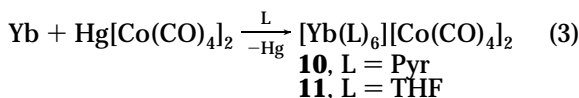$$[(Pyr)_5Yb(CH_3CN)_2] \, [Hg\{Fe(CO)_4\}_2] \cdot 2Pyr$$
$$\textbf{14}$$
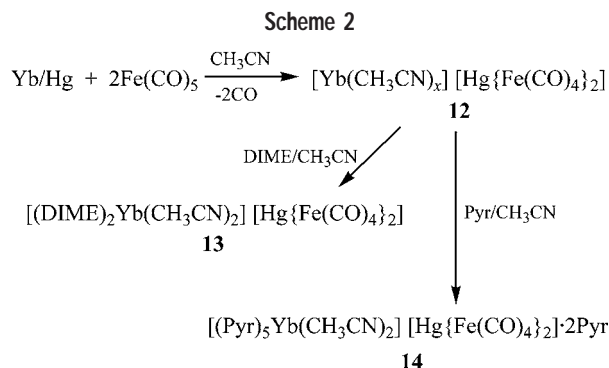
2.2. Solvent-Separated Ion Pairs. Tetracarbonylcobaltate and pentacarbonylmanganate are considered weak nucleophiles when compared to other carbonylate anions.[9] Consequently, when $Co_2(CO)_8$, $Hg[Co(CO)_4]_2$, or $Mn_2(CO)_{10}$ was combined with metallic lanthanides in the presence of strong coordinating solvents, solvent-separated ions (B of Chart 1) were isolated.[10,11]

Lanthanide/mercury amalgam reduction of $Co_2(CO)_8$ or $Mn_2(CO)_{10}$ in DME (glyme) or DIME (diglyme) causes cleavage of the M−M bond in the carbonyl dimer and produces a Ln^{2+} cation and the $[Co(CO)_4]^-$ or $[Mn(CO)_5]^-$ anion (eqs 1 and 2).[10] These anions do not adequately compete with the chelating ether solvents for binding to the Ln^{2+} ion, and the salts, $[Ln(L)_x][Co(CO)_4]_2$ (**3−5**) and $[Ln(L)_x][Mn(CO)_5]_2$ (**6−9**), are obtained:

$$Ln/Hg \ + \ Co_2(CO)_8 \xrightarrow{L} [Ln(L)_x][Co(CO)_4]_2$$
3, Ln = Sm, L = DME
4, Ln = Sm, L = DIME, $x = 3$
5, Ln = Yb, L = DIME, $x = 3$
DME = $CH_3OCH_2CH_2OCH_3$
DIME = $(CH_3OCH_2CH_2)_2O$ (1)

$$Ln/Hg \ + \ Mn_2(CO)_{10} \xrightarrow{L} [Ln(L)_x][Mn(CO)_5]_2$$
6, Ln = Sm, L = DME
7, Ln = Sm, L = DIME, $x = 3$
8, Ln = Yb, L = DIME, $x = 3$
9, Ln = Eu, L = DIME, $x = 3$
(2)
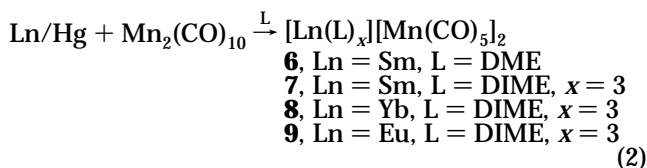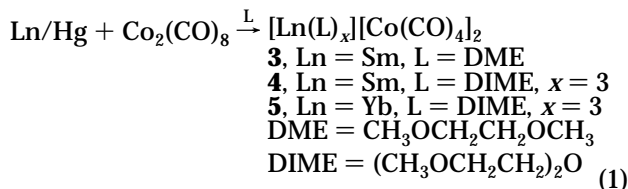
A similar result ensues in the transmetalation or metal exchange reaction of Yb and $Hg[Co(CO)_4]_2$ (eq 3).[11] During this reaction, Yb metal is oxidized to Yb(II) with concomitant reduction of Hg(II) to elemental Hg. Pyridine and THF are both relatively stronger Lewis bases than $[Co(CO)_4]^-$, and the Yb^{2+} ion is shielded from the anion by the solvent to procure $[Yb(L)_6][Co(CO)_4]_2$ (**10** and **11**):

$$Yb \ + \ Hg[Co(CO)_4]_2 \xrightarrow[-Hg]{L} [Yb(L)_6][Co(CO)_4]_2 \quad (3)$$
10, L = Pyr
11, L = THF

The solvent-separated ion pair, $[Yb(CH_3CN)_x][Hg\{Fe(CO)_4\}_2]$ (**12**), is generated from the Yb/Hg amalgam reduction of $Fe(CO)_5$ in CH_3CN (Scheme 2).[10] Compound **12** could not be crystallized in CH_3CN. However, in mixed solvents the salts $[(DIME)_2Yb(CH_3CN)_2][Hg\{Fe(CO)_4\}_2]$ (**13**) and $[(Pyr)_5Yb(CH_3CN)_2][Hg\{Fe(CO)_4\}_2]\cdot2Pyr$ (**14**) were isolated. In Schemes 1 and 2, both reductions initially gener-

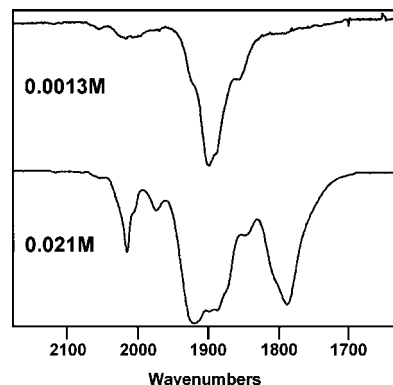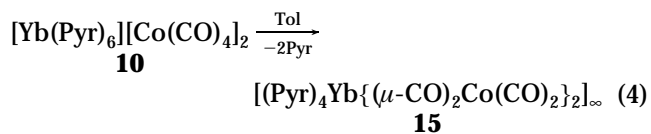**FIGURE 3.** Solution IR spectra of $[Yb(THF)_6][Co(CO)_4]_2$ (**11**) in THF as a function of concentration.

ate $[Fe(CO)_4]^{2-}$, but a Yb−Fe bonded product is not yielded in Scheme 2. The reason for this fact is that $[Fe(CO)_4]^{2-}$, a soft Lewis base, prefers the softer Lewis acid, Hg(II), over Yb(II). Consequently, Hg prevents the formation of a Yb−Fe bond.
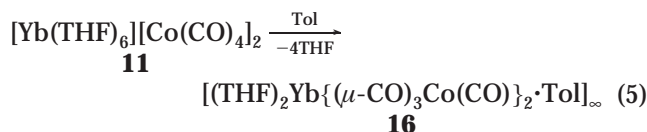
Products **3−14** are solvent-separated ion pairs in the solid state. In solution, however, the carbonyl oxygens may compete with the solvent for binding to the lanthanide cation. When the relative nucleophilicities of the carbonylate anion and solvent are comparable, this competition is expected, and an equilibrium between the ionic compound and an isocarbonyl arises. The presence of an isocarbonyl interaction is clearly evident from solution IR spectroscopy (low frequency μ-CO stretch).[12]

Solution isocarbonyl interactions with Ln(II) are prevalent for $[Co(CO)_4]^-$ or $[Mn(CO)_5]^-$ in the moderately strong donating solvents, DME and THF.[10,11] In THF, isocarbonyl associations are observed for **11**, and the strength of the interaction is a function of concentration (Figure 3).[11] Dilute solutions (0.0013 M) of **11** have primarily the solvent-separated ion (1887 cm⁻¹), but a weak contact ion pair ($[(THF)_xYb\cdots OCCo(CO)_3][Co(CO)_4]$, 1898 and 1854 cm⁻¹) also exists. More concentrated solutions (0.021 M) show the emergence of a broad low-frequency band at 1789 cm⁻¹ and several higher-frequency terminal CO stretches. Therefore, higher concentrations of **11** promote the formation of a strong carbonyl-bridged complex that is in equilibrium with the solvent-separated and weak contact ion pairs.

2.3. Isocarbonyls. Syntheses of isocarbonyls typically employ a moderately strong transition metal carbonylate nucleophile (i.e., $[CpMo(CO)_3]^-$).[9] Nonetheless, we have demonstrated that solvent-separated products formed from weak carbonylate nucleophiles may be converted with facility into isocarbonyls (C of Chart 1) utilizing a noncoordinating solvent.[11]

In toluene, salts **10** and **11** transform into the neutral isocarbonyl polymeric arrays, $[(Pyr)_4Yb\{(\mu\text{-}CO)_2Co(CO)_2\}_2]_\infty$ (**15**) and $[(THF)_2Yb\{(\mu\text{-}CO)_3Co(CO)\}_2\cdot Tol]_\infty$ (**16**) (eqs 4 and 5):[11]

$$[Yb(Pyr)_6][Co(CO)_4]_2 \xrightarrow[-2Pyr]{Tol}$$
10

$$[(Pyr)_4Yb\{(\mu\text{-}CO)_2Co(CO)_2\}_2]_\infty \quad (4)$$
15

$$[Yb(THF)_6][Co(CO)_4]_2 \xrightarrow[-4THF]{Tol}$$
11

$$[(THF)_2Yb\{(\mu\text{-}CO)_3Co(CO)\}_2 \cdot Tol]_\infty \quad (5)$$
**16**

Without the presence of other Lewis bases, the carbonyl oxygens can ligate to the Lewis acidic Yb^{2+} cations. Solution IR spectra in toluene confirm that **15** and **16** have carbonyl bridges with stretches at 1780 cm^{-1}. The carbonyl linkages are relatively weak. They are cleaved by pyridine and THF to regenerate the parent solvent-separated ions, **10** and **11**. Compound **16** is not converted back to **11** completely because the solvent-separated ions exist in equilibrium with the weak contact ion pair and an isocarbonyl species.

Molecular structures of **15** and **16** are distinct. Each {Co(CO)$_4$} moiety in **15** bridges through two carbonyls to two Yb(II) atoms (Figure 4). The Yb atoms, in turn, are bonded to four isocarbonyl oxygens. In contrast, three carbonyls on each {Co(CO)$_4$} unit in **16** are involved in a bridging interaction, and there are six isocarbonyl connections per Yb(II) (Figure 5). The consequence of these Yb−OC−Co linkages is a 2-D sheetlike array. By attaching "eight-membered" rings (four Yb and four Co atoms) together, **15**'s structure is created. "Four-membered" ring building blocks are incorporated into the sheet of **16**. Complexes **15** and **16** belong to a rare class of Ln−M carbonyl extended polymeric structures, only three others of which have been structurally characterized (**1**, **2**, and one prepared by Andersen et al.[1d]).

3. Ln(II)−M Cyanides

In conjunction with the Ln(II)−M carbonyl studies, we investigated heterometallic combinations of Ln(II) with group 10 cyanometalates. A convenient route toward Ln(II)−M cyanides is a metathesis reaction between a Ln(II) salt and a cyanometalate salt (i.e., [M(CN)$_4$]$^{2-}$). Highly polar solvents, such as DMF (*N,N*-dimethylformamide), are necessary to solubilize the reactants. X-ray structural studies demonstrate that cyanide functions as a bidentate ligand to construct cyanide bridges, Ln−NC−M. The following two complexes are believed to be the first reported Ln(II)−M cyanide substances.[13]

Reactions of EuCl$_2$ and K$_2$[M(CN)$_4$] (M = Ni, Pt) in DMF afford {(DMF)$_4$Eu[M(CN)$_4$]}$_4$ (**17** and **18**; eq 6):[13]

$$EuCl_2 + K_2[M(CN)_4] \xrightarrow[-2KCl]{DMF} \{(DMF)_4Eu[M(CN)_4]\}_\infty$$
17, M = Ni
18, M = Pt
(6)
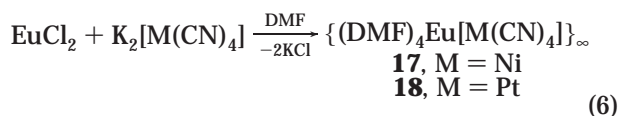
Compounds **17** and **18** are isostructural (Figure 6). Cyanide linkages manufacture a 1-D infinite ladder. Three of the four {M(CN)$_4$} cyanides partake in bridging cyanide interactions to three different Eu(II) atoms. These junctures frame the ladder uprights and rungs. We believe that **17** and **18** are the first structural examples of a tetracyanometalate utilizing three of the four cyanides as bidentate ligands.
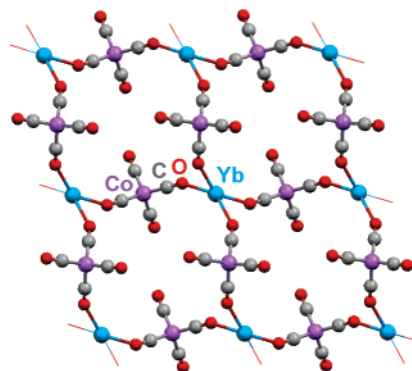
FIGURE 4. 2-D sheetlike network of [(Pyr)$_4$Yb{(μ-CO)$_2$Co(CO)$_2$}$_2$]$_\infty$ (**15**).
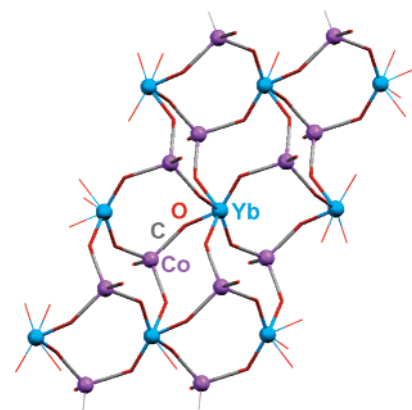
FIGURE 5. 2-D sheetlike array of [(THF)$_2$Yb{(μ-CO)$_3$Co(CO)}$_2$·Tol]$_\infty$ (**16**). Carbon and oxygen atoms are drawn as capped sticks for clarity.
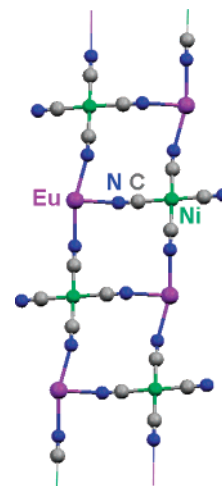
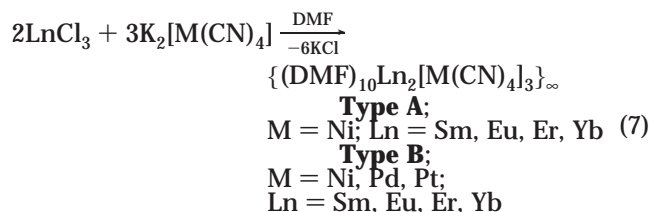**FIGURE 6.** Structure of the 1-D ladder of {(DMF)$_4$Eu[Ni(CN)$_4$]}$_\infty$ (**17**).

4. Ln(III)−M Cyanides

Application studies of Ln(II)−M systems are limited to Sm, Eu, and Yb because the +2 oxidation state is unstable for the other lanthanides under normal conditions.[14] Conversely, trivalent lanthanides are thermodynamically stable and are easy to manipulate. Even though the harder Lewis acidity of Ln^{3+} compared to Ln^{2+} discourages the formation of Ln−M direct bonds in our systems, the ionic ligand [CN]$^-$ binds to Ln through N more strongly than O of CO. Furthermore, no linkage isomerism (Ln−NC−M, Ln−

CN−M) is observed in the complexes since the soft Lewis basic carbon end of [CN]⁻ prefers the softer Lewis acidic M(II) ion. Cyanide is a better choice for preparing stable polymeric structures, and the extended arrays are conducive for catalytic[4,15] and materials research. These advantages encouraged us to develop a structurally diverse assortment of cyanide-bridged Ln(III)−M(groups 10, 11) compounds.

4.1. Ln(III)−M(Group 10) Cyanide Systems and Structural Types. We prepared a series of Ln(III)−M cyanide bimetallic complexes by means of metathesis reactions of LnCl₃ with $K_2[M(CN)_4]$ in DMF. The ideal reactant ratio of Ln and group 10 metal is 2:3, and 1-D polymeric products with the general formula $\{(DMF)_xLn_2[M(CN)_4]_3\}_\infty$ (Ln = La, Ce, Sm, Eu, Er, Yb; M = Ni, Pd, Pt; x = 10, 12) were isolated.[16−19] The compounds have different structural types, and the factors that govern their formations were identified. These kinds of complexes are proven catalytic precursors.[4,15] A change in the metathesis reaction ratio to 1:1 produced 1-D arrays $\{(L)_xLn[Ni(CN)_4]Cl\}_\infty$ (Ln = Sm, Yb; L = DMF, DMA (*N,N*-dimethylacetamide); x = 4, 5), which have a remaining chloride ion bonded to the Ln(III) center.[17] On the other hand, 1:2 ratios of LnCl₃ and $K_2[M(CN)_4]$ or $[NH_4]_2[Pt(CN)_4]$ generated more complicated sheet and columnlike structures, $\{(DMF)_{10}Ln_2[M(CN)_4]_3 \cdot K_2(DMF)_4[M(CN)_4]\}_\infty$ (Ln = Eu, Yb; M = Ni, Pt) and $\{[NH_4][(DMF)_4Yb[Pt(CN)_4]_2]\}_\infty$.[20]

4.1.1. 1-D Complexes with Type A, Type B, and Type C Structures. The Ln(III)−M cyanides $\{(DMF)_{10}Ln_2[M(CN)_4]_3\}_\infty$ (type A, type B; Ln = Sm, Eu, Er, Yb; M = Ni, Pd, Pt) were quantitatively prepared via metathesis reactions of anhydrous LnCl₃ and $K_2[M(CN)_4]$ in 2:3 molar ratios in DMF at room temperature (eq 7):[16−18]

$$2LnCl_3 + 3K_2[M(CN)_4] \xrightarrow[-6KCl]{DMF}$$
$$\{(DMF)_{10}Ln_2[M(CN)_4]_3\}_\infty$$

Type A;
M = Ni; Ln = Sm, Eu, Er, Yb   (7)
Type B;
M = Ni, Pd, Pt;
Ln = Sm, Eu, Er, Yb

These complexes crystallize as 1-D linear single-strands (structural type A, Figure 7) or double-strands (structural type B, Figure 8), depending upon the conditions employed. The single-strand type A structures consist of cyanide-bridged, "diamond"-shaped Ln₂Ni₂ cores, which are linked together through *trans*-cyanide bridging [Ni-(CN)₄]²⁻ anions. In comparison, the double-strand type B structures have cyanide-bridged hexagonal units that include Ln₄M₄ cores. Both structural classes possess the same asymmetric unit $\{[M(CN)_2]Ln(DMF)_5[M(CN)_4]\}$ (**I** in Scheme 3) and the same repeating unit $\{[M(CN)_4]-(DMF)_5Ln[M(CN)_4]Ln(DMF)_5[M(CN)_4]\}$ (**II** in Scheme 3). The difference between type A (**III**) and type B (**IV**) arises from the distinct spatial combinations of the repeating units (Scheme 3). Type A structures form instantly when the solution is supersaturated. Type B structures assemble upon slow crystallization. Furthermore, type A crystals can convert to type B crystals at room temperature in days.
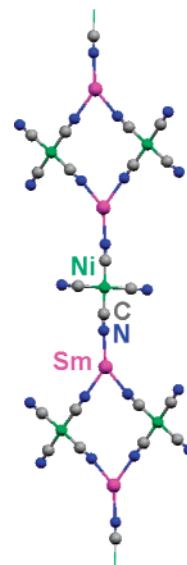

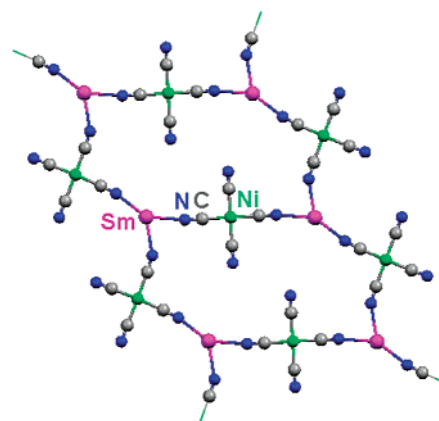**FIGURE 7.** Type A 1-D single-strand chain of $\{(DMF)_{10}Ln_2[M(CN)_4]_3\}_\infty$ (Ln = Sm, M = Ni).

FIGURE 8. Type B 1-D double-strand array of $\{(DMF)_{10}Ln_2[M(CN)_4]_3\}_\infty$ (Ln = Sm, M = Ni).

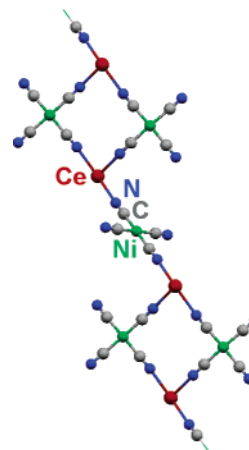**FIGURE 9.** Type C 1-D zigzag chain of $\{(DMF)_{12}Ln_2[M(CN)_4]_3\}_\infty$ (Ln = Ce, M = Ni).

On the basis of this result, the construction of type A compounds appears to be kinetically favored, whereas type B complexes are believed to be thermodynamically favored. This type A to B transformation occurs only for Ln−Ni (Ln = Sm, Eu, Er, Yb) complexes. The type B

Scheme 3. Building Blocks of {(DMF)₁₀Ln₂[M(CN)₄]₃}∞ (Type A and Type B) Compounds; Formation of (a) the Repeating Unit (II) from the Asymmetric Unit (I), (b) Type A Structures (III) from the Repeating Unit, and (c) Type B Structures (IV) from the Repeating Unit

(a)

(I) Asymmetric unit   **(II) Repeating unit**

(b)

(III) Type A

(c)

(IV) Type B
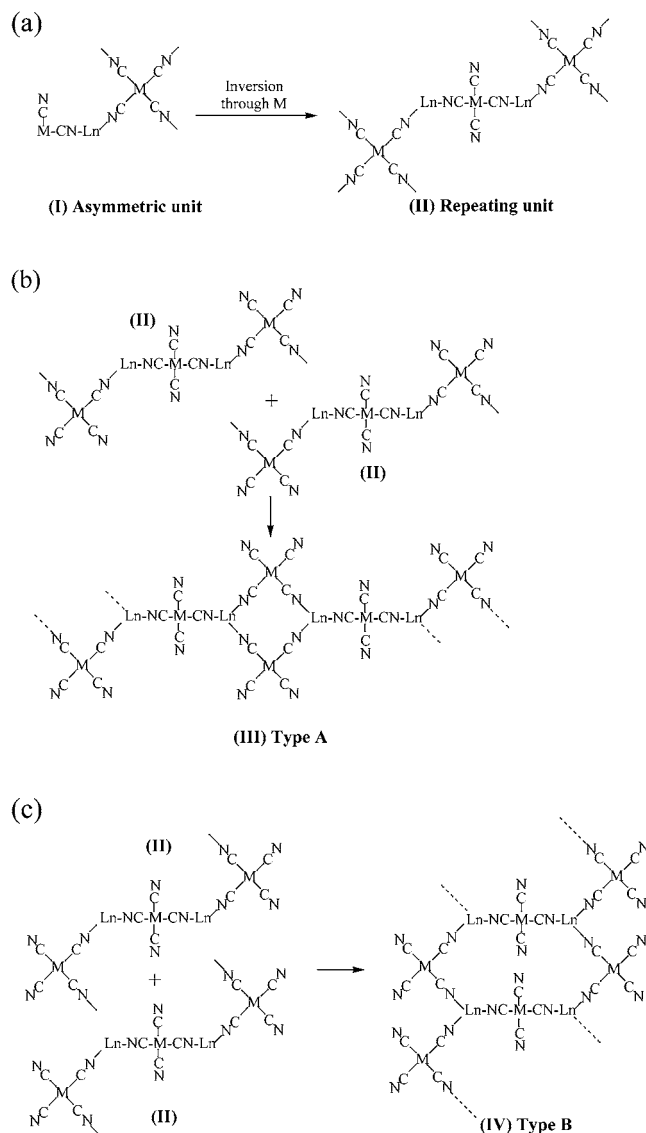
structure appears to be exclusively created when the transition metal is Pd or Pt.

Metathesis reactions involving LnCl₃ reagents with larger Ln³⁺ ionic radii (Ln = La, Ce) produced a new 1-D zigzag chainlike array, {(DMF)₁₂Ln₂[M(CN)₄]₃}∞ (Ln = La, Ce; M = Ni, Pd), designated as type C (eq 8, Figure 9):[18,19]

$$2LnCl_3 + 3K_2[M(CN)_4] \xrightarrow[-6KCl]{DMF} \{(DMF)_{12}Ln_2[M(CN)_4]_3\}_\infty$$

Type C;
Ln = La, Ce; M = Ni, Pd

(8)
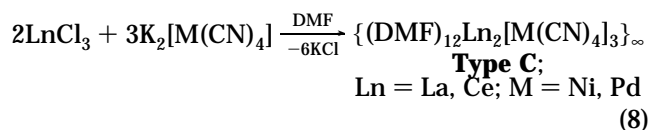
Even though the Ln₂M₂ core is "diamond"-shaped, the [M(CN)₄]²⁻ linkages between the cores in type C complexes are different from those in type A structures. The Ln³⁺ coordination number in type C complexes is 9, and in type A it is 8. This difference in coordination geometries causes a distortion of the N−Ln−N angle and accounts
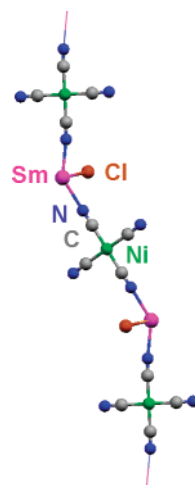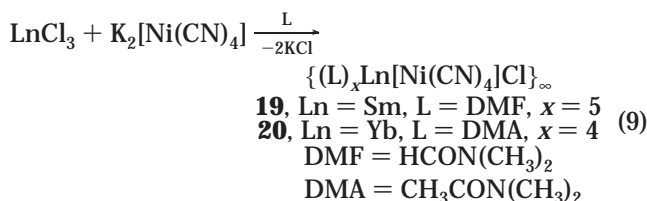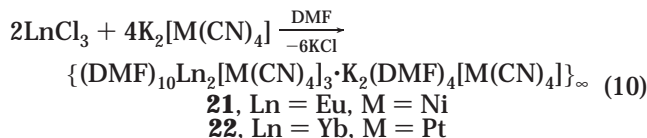
FIGURE 10. 1-D zigzag chain of {(DMF)₅Sm[Ni(CN)₄]Cl}∞ (**19**).

for the formation of a zigzag type C chain rather than a linear type A array.

4.1.2. 1-D Chloride Complexes. Reactions utilizing equal molar amounts of LnCl₃ (Ln = Sm, Yb) and K₂[Ni(CN)₄] in DMF or DMA yielded the 1-D chainlike arrays {(DMF)₅-Sm[Ni(CN)₄]Cl}∞ (**19**, Figure 10) and {(DMA)₄Yb[Ni(CN)₄]-Cl}∞ (**20**) (eq 9).[17] The cyanometalate [M(CN)₄]²⁻ is connected to Ln³⁺ cations through two *trans*-cyanide groups. This results in 1-D arrays that are simpler than the type A, B, and C structures, which combine *trans*- and *cis*-cyanide bridges to yield LnₓMₓ cores:

$$LnCl_3 + K_2[Ni(CN)_4] \xrightarrow[-2KCl]{L}$$

$$\{(L)_xLn[Ni(CN)_4]Cl\}_\infty$$

19, Ln = Sm, L = DMF, $x = 5$
20, Ln = Yb, L = DMA, $x = 4$ (9)
DMF = HCON(CH₃)₂
DMA = CH₃CON(CH₃)₂

4.1.3. Extended Arrays with K⁺ and NH₄⁺ Cations. The reaction between anhydrous LnCl₃ (Ln = Eu, Yb) and K₂-[M(CN)₄] (M = Ni, Pt) in a 1:2 molar ratio in DMF produced {(DMF)₁₀Ln₂[M(CN)₄]₃·K₂(DMF)₄[M(CN)₄]}∞ (**21, 22**; eq 10):[20]

$$2LnCl_3 + 4K_2[M(CN)_4] \xrightarrow[-6KCl]{DMF}$$

$$\{(DMF)_{10}Ln_2[M(CN)_4]_3 \cdot K_2(DMF)_4[M(CN)_4]\}_\infty \quad (10)$$

21, Ln = Eu, M = Ni
22, Ln = Yb, M = Pt

Complexes **21** and **22** consist of neutral, 2-D, puckered sheets with the formula {(DMF)₁₀Ln₂[M(CN)₄]₃}∞ (Figure 11). Although these sheets have the same formulation as type A and B compounds, the repeating units are different. The hexagonal Ln₆M₆ cores, which share common edges, have Ln³⁺ cations positioned on the corners and [M(CN)₄]²⁻ anions on the edges. In relation to the two types of cyanide bridges and the 1-D structures of type A, B, and C complexes, **21** and **22** possess only *trans*-cyanide connections between the Ln and M centers, which cause the production of more complicated 2-D frameworks. Interstitial K₂(DMF)₄[M(CN)₄] units are located between these layers (Figure 12). The [M(CN)₄]²⁻ groups are positioned
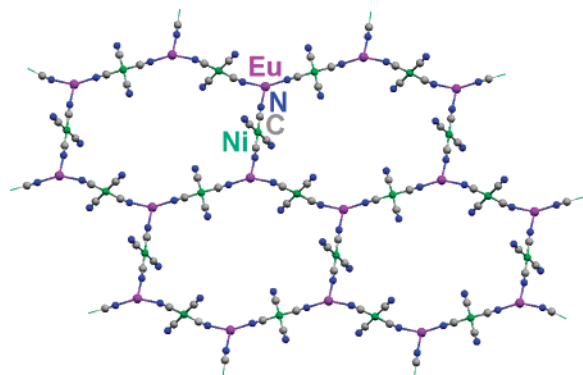
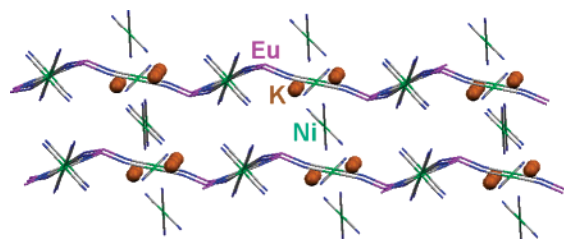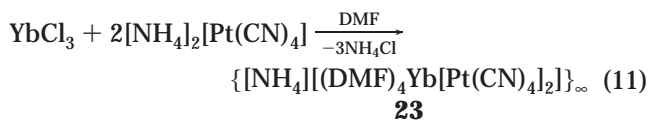**FIGURE 11.** 2-D puckered sheet, $\{(DMF)_{10}Eu_2[Ni(CN)_4]_3\}_\infty$, in $\{(DMF)_{10}Eu_2[Ni(CN)_4]_3 \cdot K_2(DMF)_4[Ni(CN)_4]\}_\infty$ (**21**).

FIGURE 12. Cross-section showing the interstitial $K_2(DMF)_4[Ni(CN)_4]$ units between the sheets of **21**. All atoms except potassiums are drawn as capped sticks.

above and below the sheets, approximately perpendicular to the sheets, and along the centers of the hexagons. Each anion is related to four K^+ cations through weak bridging cyanide interactions. Each K^+ cation is associated with two interstitial $[M(CN)_4]^{2-}$ anions and with the terminal cyanide of a $[M(CN)_4]^{2-}$ anion in the hexagonal ring. The K_2-$(DMF)_4[M(CN)_4]$ units, which serve as spacers between the sheets, appear to be a critical requirement for the creation of the sheet.

In a similar metathesis procedure, $YbCl_3$ was reacted with 2 equiv of $[NH_4]_2[Pt(CN)_4]$ in DMF, and $\{[NH_4][(DMF)_4$-$Yb[Pt(CN)_4]_2]\}_\infty$ (**23**) was generated (eq 11):[20]

$$YbCl_3 + 2[NH_4]_2[Pt(CN)_4] \xrightarrow[-3NH_4Cl]{DMF}$$
$$\{[NH_4][(DMF)_4Yb[Pt(CN)_4]_2]\}_\infty \quad (11)$$
$$\textbf{23}$$

Product **23** is comprised of negatively charged columns, $\{[(DMF)_4Yb[Pt(CN)_4]_2]^-\}_\infty$ (Figure 13). The columns are constructed from stacked Yb_2Pt_2 squares that are linked by $[Pt(CN)_4]^{2-}$ anions. Larger Yb_4Pt_4 "eight-membered" rings are perpendicular to the squares. In contrast to **21** and **22**, all bridging cyanide connections occur only through *cis*-cyanide groups. The columns are bundled together by N−H⋯N−C hydrogen bonds between NH_4^+ cations and terminal cyanides from the columns (Figure 14). Each NH_4^+ cation is bound to three columns, and overall, this hydrogen bonding creates a 3-D array.

4.1.4. An Oxo-Hydroxo-Lanthanide Cluster. A new and unexpected type of Ln(III)−M(group 10) cyanide was prepared by the redox reaction between $YbCl_2$ and $K_2[Pd$-$(CN)_4] \cdot H_2O$ (Scheme 4).[21] The water of crystallization causes oxidation of Yb^{2+} to Yb^{3+} and the formation of O^{2-},
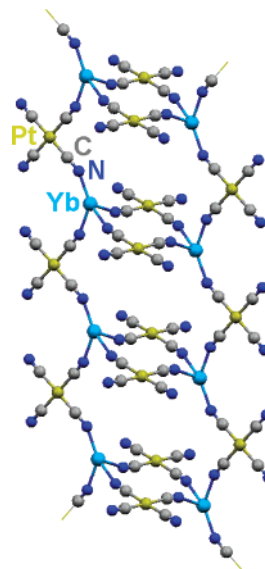

FIGURE 13. Side view of a negatively charged column, $\{[(DMF)_4Yb$-$[Pt(CN)_4]_2]^-\}_\infty$, in $\{[NH_4][(DMF)_4Yb[Pt(CN)_4]_2]\}_\infty$ (**23**).
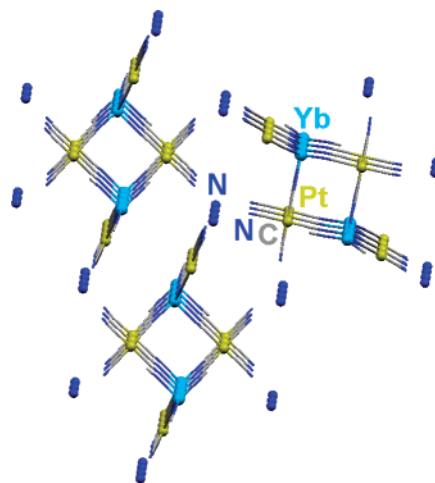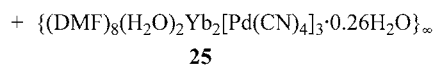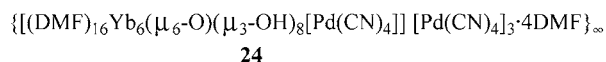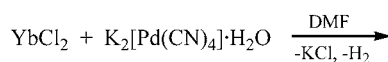

FIGURE 14. View looking down the columns of **23**. Each interstitial NH_4^+ cation is associated with three columns. Hydrogen atoms on NH_4^+ cations are omitted for clarity. Cyanide carbon and nitrogen atoms are drawn as capped sticks.

Scheme 4

$$YbCl_2 + K_2[Pd(CN)_4] \cdot H_2O \xrightarrow[-KCl, -H_2]{DMF}$$

$$\{[(DMF)_{16}Yb_6(\mu_6\text{-}O)(\mu_3\text{-}OH)_8[Pd(CN)_4]] [Pd(CN)_4]_3 \cdot 4DMF\}_\infty$$
$$\textbf{24}$$

$$+ \{(DMF)_8(H_2O)_2Yb_2[Pd(CN)_4]_3 \cdot 0.26H_2O\}_\infty$$
$$\textbf{25}$$

OH^-, and H_2. Two ionic products $\{[(DMF)_{16}Yb_6(\mu_6\text{-}O)(\mu_3\text{-}$ $OH)_8[Pd(CN)_4]][Pd(CN)_4]_3 \cdot 4DMF\}_\infty$ (**24**) and $\{(DMF)_8(H_2O)_2$-$Yb_2[Pd(CN)_4]_3 \cdot 0.26H_2O\}_\infty$ (**25**) are formed. The structure of **25** belongs to the type A family. Compound **24** is unique because it is composed of an oxo-hydroxo-lanthanide cluster core, $\{Yb_6(\mu_6\text{-}O)(\mu_3\text{-}OH)_8\}$ (Figure 15). This core has an interstitial O^{2-} anion that is octahedrally coordinated to six Yb^{3+} cations. Eight OH^- anions cap each triangular face of the octahedron. Two Yb^{3+} cations in the
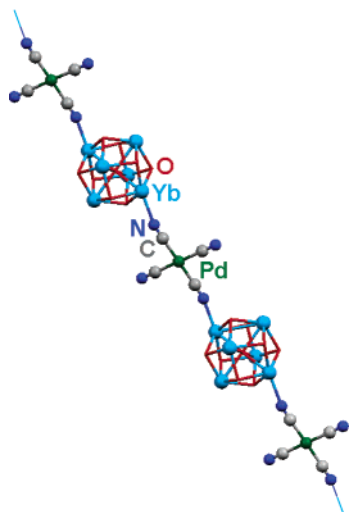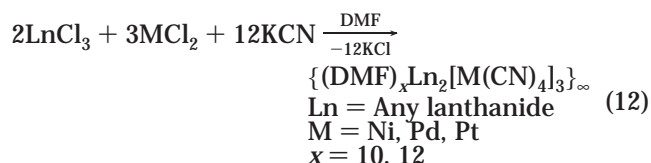
FIGURE 15. Structure of the 1-D cationic chain, $\{[(DMF)_{16}Yb_6(\mu_6\text{-}O)(\mu_3\text{-}OH)_8[Pd(CN)_4]]^{6+}\}_\infty$, in $\{[(DMF)_{16}Yb_6(\mu_6\text{-}O)(\mu_3\text{-}OH)_8[Pd(CN)_4]][Pd\text{-}(CN)_4]_3\cdot 4DMF\}_\infty$ (**24**). Oxygen atoms are drawn as capped sticks and hydroxide hydrogens are omitted for clarity.

cluster are each bound to a cyano nitrogen of $[Pd(CN)_4]^{2-}$. Individual clusters are coupled by *trans*-cyanide linkages with $[Pd(CN)_4]^{2-}$ units. The outcome is a 1-D cationic chain, $\{[(DMF)_{16}Yb_6(\mu_6\text{-}O)(\mu_3\text{-}OH)_8[Pd(CN)_4]]^{6+}\}_\infty$. Non-bridging $[Pd(CN)_4]^{2-}$ anions balance the charge of the cationic chain. Despite the unusual nature of this reaction, it is reproducible. If $YbCl_3$ is used in lieu of $YbCl_2$ in the presence of H_2O, a cluster compound is not observed. Instead, a Ln(III)−M cyanide complex, such as **25**, is produced. The Yb(II) reagent appears to be necessary for the construction of the oxo-hydroxo-Yb_6 cluster.

4.1.5. A Simplified Metathesis Reaction Procedure. Though we have extensively employed $K_2[M(CN)_4]$ (M = Ni, Pd, Pt) in our metathesis reactions, it is an expensive reagent. It is also difficult to completely remove water of crystallization from the hydrate. A simplified and more economic route that appears to be generally applicable to all Ln(III)−M(group 10) cyanides was developed (eq 12).[18] This pathway affords the same products as the $K_2[M(CN)_4]$ reaction in a clean and quantitative fashion:

$$2LnCl_3 + 3MCl_2 + 12KCN \xrightarrow[-12KCl]{DMF}$$
$$\{(DMF)_xLn_2[M(CN)_4]_3\}_\infty$$
$$\text{Ln = Any lanthanide} \quad (12)$$
$$\text{M = Ni, Pd, Pt}$$
$$x = 10, 12$$

4.2. Ln(III)−M(Group 11) Cyanide Systems and Structural Types. Recently, our structural and chemical studies of Ln(III)−M cyanides were extended from group 10 transition metals to group 11 metals.[22] Through two different types of metathesis reactions, two unique Gd(III)−Cu(I) cyanide complexes were prepared. One is a 3-D inclusion compound, which has an anionic $\{[Cu_6(CN)_9]^{3-}\}_\infty$ lattice and sequestered $[Gd(DMF)_8]^{3+}$ cations. The other is a 2-D layer array, $\{Gd_2(DMF)_8Cu_4(CN)_{10}\}_\infty$. Not only are these two compounds structurally dissimilar, but they also represent new Ln(III)−M cyanide structural classes that were not previously observed.
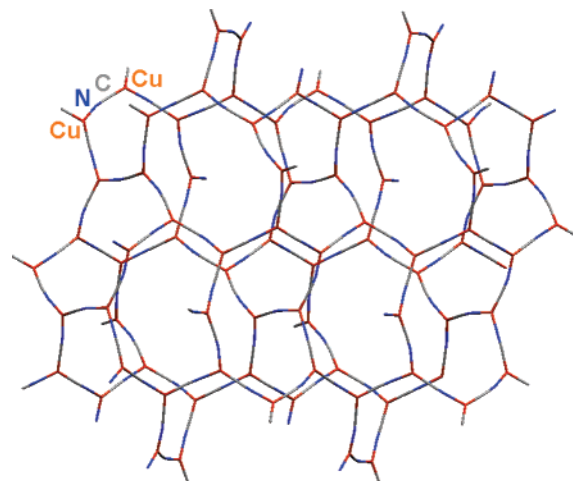

FIGURE 16. 3-D anionic network, $\{[Cu_6(CN)_9]^{3-}\}_\infty$, of $\{[Gd(DMF)_8]\text{-}[Cu_6(CN)_9]\cdot 2DMF\}_\infty$ (**26**) with four vacant pockets.

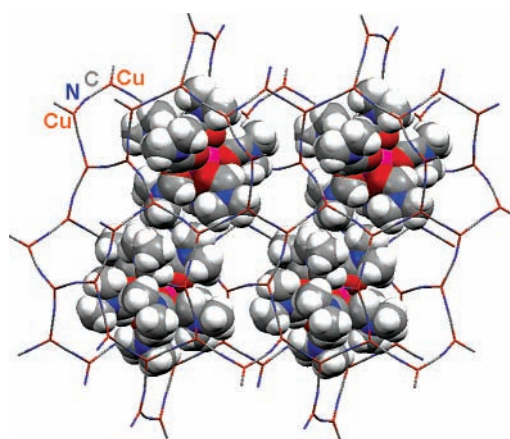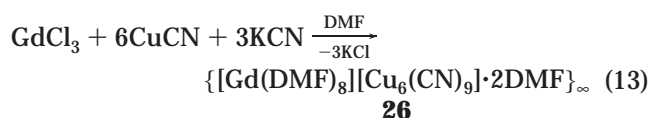**FIGURE 17.** Four trapped $[Gd(DMF)_8]^{3+}$ cations within the anionic cage of **26**. The cations are drawn as Spacefill.

A three component metathesis reaction involving $GdCl_3$, CuCN, and KCN in DMF at room temperature created the 3-D inclusion complex, $\{[Gd(DMF)_8][Cu_6(CN)_9]\cdot 2DMF\}_\infty$ (**26**; eq 13):[22]

$$GdCl_3 + 6CuCN + 3KCN \xrightarrow[-3KCl]{DMF}$$
$$\{[Gd(DMF)_8][Cu_6(CN)_9]\cdot 2DMF\}_\infty \quad (13)$$
$$\textbf{26}$$

The anionic 3-D network, $\{[Cu_6(CN)_9]^{3-}\}_\infty$, is assembled from Cu−NC−Cu cyanide bridges (Figure 16). Each Cu(I) atom is bonded to three cyanide groups. The anionic framework possesses pockets, each of which is occupied by a $[Gd(DMF)_8]^{3+}$ cation and two DMF solvent molecules (Figure 17). Compound **26** is a host−guest molecule since the $[Gd(DMF)_8]^{3+}$ cation (approximate diameter is >12.0 Å) is securely enclosed within the Cu−CN lattice (the width of the biggest window is <10.2 Å). Although other ionic inclusion systems are known, **26** is the first example of an encapsulated lanthanide ion in a charged cage.

The metathesis reaction in eq 13 was modified by initially preparing and isolating $K[Cu(CN)_2]$ (eq 14a), which was then reacted with $GdCl_3$ (eq 14b).[22] To our surprise,

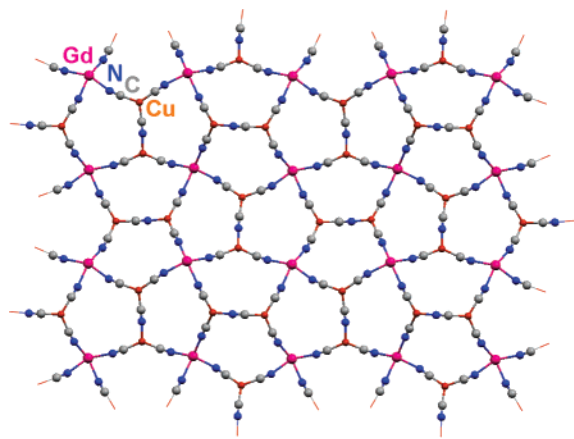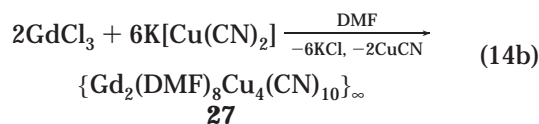**FIGURE 18.** 2-D extended layer of $\{Gd_2(DMF)_8Cu_4(CN)_{10}\}_\infty$ (**27**).

a new Gd(III)−Cu(I) cyanide, $\{Gd_2(DMF)_8Cu_4(CN)_{10}\}_\infty$ (**27**),was afforded:

$$CuCN + KCN \xrightarrow{DMF} K[Cu(CN)_2] \qquad (14a)$$

$$2GdCl_3 + 6K[Cu(CN)_2] \xrightarrow[-6KCl,\ -2CuCN]{DMF}$$
$$\{Gd_2(DMF)_8Cu_4(CN)_{10}\}_\infty \qquad (14b)$$
$$\mathbf{27}$$

Product **27** is a 2-D puckered layer structure that is comprised of "five-membered" ring building blocks (Figure 18). The Gd_2Cu_3 pentagons are constructed from two different cyanide linkages, Gd−NC−Cu and Cu−NC−Cu. Through these bridges, each Cu is bound to two Gd atoms and one Cu, and each Gd is connected to four Cu atoms. To our knowledge, this is the first example of a cyanide-bridged Ln(III)−M array that is based upon pentagonal repeating units.

Clearly, the distinct reaction procedures of eqs 13 and 14 account for the variation in products. In eq 13, the low solubility of CuCN in DMF results in a low concentration of $K[Cu(CN)_2]$ at any given time. This favors the formation of the solvated $[Gd(DMF)_8]^{3+}$ cation over Gd−NC−Cu bridges. Such a situation would allow for the slow assembly of the Cu−CN anionic network around the solvated Gd^{3+} cation. (Complex **26** requires several weeks for crystallization.) On the other hand in eq 14, $K[Cu(CN)_2]$ has significant solubility in DMF. The salt $K[Cu(CN)_2]$ has Cu−NC−Cu linkages and terminal cyanides, which can couple to Gd(III) to yield the layer structure **27**. (Complex **27** crystallizes in about 1 day.)

5. Conclusions and Outlook

In this Account, we outlined our work on lanthanide−transition-metal systems. The themes of this research were the development of synthetic methodology for novel Ln−M compounds and the investigation of their structures. Our synthetic findings demonstrate that most divalent and trivalent lanthanides formed heterometallic complexes with middle or late transition metals. Transition-metal carbonyls and cyanides are convenient starting materials for these mixed-metal products. These new

Ln−M combination substances exhibit diversity of structure. Compounds derived from $[M(CO)_y]^{n-}$ fall into three classes of Ln−M interactions, metal−metal bonded species, ion pairs, and isocarbonyls. The Ln−M bonded complexes possess 1-D or 2-D structures, the ion pairs are discrete molecules, and isocarbonyls are 2-D layers. The Ln−M cyanide systems have linkages that create 1-D, 2-D, and 3-D polymeric arrays. The latter complexes function as heterogeneous catalyst precursors. Although we have prepared numerous Ln−M compounds, our studies are by no means complete. We are currently extending our Ln(III)−Cu(I) cyanide chemistry and are interested in the practical application of these Ln−Cu substances and the Ln(II)−M carbonyls as catalyst precursors. The Ln(III)−M(group 10) cyanides are the subject of magnetic materials research.

References

(1) (a) James, C.; Willand, P. S. The Rare Earth Cobalticyanide. *J. Am. Chem. Soc.* **1916**, *38*, 1497−1500. (b) See, for example: Bailey, W. E.; Williams, R. J.; Milligan, W. O. The Crystal Structure of LaFe(CN)_6·5H_2O. *Acta Crystallogr.* **1973**, *B29*, 1365−1368. (c) See, for example: Crease, A. E.; Legzdins, P. The Lewis Acidity of Organolanthanides. The Interaction of Cyclopentadienyl-Lanthanides with some Carbonyl and Nitrosyl Complexes. *J. Chem. Soc., Dalton Trans.* **1973**, 1501−1507. (d) See, for example: Boncella, J. M.; Andersen, R. A. Bis(pentamethylcyclopentadienyl)ytterbium(II) as a Lewis Acid and Electron-Transfer Ligand. Preparation and Crystal Structures of [Yb(Me_5C_5)_2(μ-CO)_xMn-(CO)_{5−x}]_y (x, y = 2; x = 3, y = ∞). *Inorg. Chem.* **1984**, *23*, 432−437.

(2) See ref 22 for citations to selected applications in materials science and catalysis.

(3) (a) Marianelli, R. S.; Durney, M. T. Tris(tetracarbonyl)tetrakis-(tetrahydrofuran)erbium. *J. Organomet. Chem.* **1971**, *32*, C41−C43. (b) Magomedov, G. K.-I.; Voskoboinikov, A. Z.; Chuklanova, E. B.; Gusev, A. I.; Beletskaya, I. P. Synthesis and Molecular Structure of Luteium-Ruthenium Complex (C_4H_8O)(η^5-C_5H_5)_2LuRu-(CO)_2(η^5-C_5H_5). *Metalloorg. Khim.* **1990**, *3*, 706−707.

(4) Rath, A.; Aceves, E.; Mitome, J.; Liu, J.; Ozkan, U. S.; Shore, S. G. Application of {(DMF)_10Ln_2[Pd(CN)_4]_3}_∞ (Ln = Yb, Sm) as Lanthanide-Palladium Catalyst Precursors Dispersed on Sol-Gel-TiO_2 in the Reduction of NO by Methane in the Presence of Oxygen. *J. Mol. Catal. A* **2001**, *165*, 103−111.

(5) Deng, H.; Shore, S. G. Direct Yb−Fe Interaction in an Organometallic "Ladder Polymer": Synthesis and Structure of {[(CH_3-CN)_3YbFe(CO)_4]_2·CH_3CN}_∞. *J. Am. Chem. Soc.* **1991**, *113*, 8538−8540.

(6) Deng, H.; Chun, S.-H.; Florian, P.; Grandinetti, P. J.; Shore, S. G. Direct Lanthanide-Transition Metal Interactions: Synthesis of (NH_3)_2YbFe(CO)_4 and Crystal Structures of {[(CH_3CN)_3YbFe(CO)_4]_2·CH_3CN}_∞ and [(CH_3CN)_3YbFe(CO)_4]_∞. *Inorg. Chem.* **1996**, *35*, 3891−3896.

(7) For the sake of clarity, solvent ligands and solvent molecules of crystallization have been omitted from those figures that depict compound structure. The exception is Figure 17.

(8) (a) Macdonald, C. L. B.; Cowley A. H. A Theoretical Study of Free and Fe(CO)_4-Complexed Borylenes (Boranediyls) and Heavier Congeners: The Nature of the Iron-Group 13 Element Bonding. *J. Am. Chem. Soc.* **1999**, *121*, 12113−12126. (b) Bursten, B. E.; Novo-Gradac, K. J. Metal−Metal Bonds Involving the f-Elements. 2. Nature of the Bonding in (η^5-C_5H_5)_2(I)M-Ru(η^5-C_5H_5)(CO)_2 (M = Zr, Th) Complexes. *J. Am. Chem. Soc.* **1987**, *109*, 904−905.

(9) Dessy, R. E.; Pohl, R. L.; King, R. B. Organometallic Electrochemistry. VII. The Nucleophilicities of Metallic and Metalloidal Anions Derived from Metals of Groups IV, V, VI, VII, and VIII. *J. Am. Chem. Soc.* **1966**, *88*, 5121−5124.

(10) White, J. P., III; Deng, H.; Boyd, E. P.; Gallucci, J.; Shore, S. G. Coordination Geometries of Solvated Ln(II) Ions: Molecular Structures of the Cationic Species [(DIME)_3Ln]^{2+} (DIME = Diethylene Glycol Dimethyl Ether; Ln^{2+} = Sm, Yb), [(DIME)_2Yb(CH_3-CN)_2]^{2+}, [(DIME)Yb(CH_3CN)_5]^{2+}, and [(C_5H_5N)_5Yb(CH_3CN)_2]^{2+}. *Inorg. Chem.* **1994**, *33*, 1685−1694.

(11) Plečnik, C. E.; Liu, S.; Liu, J.; Chen, X.; Meyers, E. A.; Shore, S. G. Lanthanide–Transition-Metal Carbonyl Complexes. 1. Syntheses and Structures of Ytterbium(II) Solvent-Separated Ion Pairs and Isocarbonyl Polymeric Arrays of Tetracarbonylcobaltate. *Inorg. Chem.* **2002**, *41*, 4936–4943.

(12) See, for example: Darensbourg, M. Y. Ion Pairing Effects on Transition Metal Carbonyl Anions. *Prog. Inorg. Chem.* **1985**, *33*, 221–274.

(13) Knoeppel, D. W.; Shore, S. G. Unusual One-Dimensional Ladder Structures Containing Divalent Europium and the Tetracyano-metalates Ni(CN)$_4^{2-}$ and Pt(CN)$_4^{2-}$. *Inorg. Chem.* **1996**, *35*, 5328–5334.

(14) McClure, D. S.; Kiss, Z. Spectra of the Bivalent Rare-Earth Ions in Cubic Crystals. *J. Chem. Phys.* **1963**, *39*, 3251–3257.

(15) Shore, S. G.; Ding, E.; Park, C.; Keane, M. A. Vapor Phase Hydrogenation of Phenol over Silica Supported Pd and Pd–Yb Catalysts. *Catal. Commun.* **2002**, *3*, 77–84.

(16) Knoeppel, D. W.; Shore, S. G. Cyanide-Bridged Lanthanide-Transition Metal One-Dimensional Arrays {(DMF)$_{10}$Yb$_2$[Ni(CN)$_4$]$_3$}$_∞$ and {(DMF)$_{10}$Yb$_2$[Pt(CN)$_4$]$_3$}$_∞$. *Inorg. Chem.* **1996**, *35*, 1747–1748.

(17) Knoeppel, D. W.; Liu, J.; Meyers, E. A.; Shore, S. G. Heterometallic One-Dimensional Arrays Containing Cyanide-Bridged Lanthanide-(III) and Transition Metals. *Inorg. Chem.* **1998**, *37*, 4828–4837.

(18) Liu, J.; Knoeppel, D. W.; Liu, S.; Meyers, E. A.; Shore, S. G. Cyanide-Bridged Lanthanide(III)-Transition Metal Extended Ar-rays: Interconversion of One-Dimensional Arrays from Single-Strand (Type A) to Double-Strand (Type B) Structures. Complexes of a New Type of Single-Strand Array (Type C). *Inorg. Chem.* **2001**, *40*, 2842–2850.

(19) Lim, S. Part I. Syntheses and Characterization of Hydrogen-Bridged Lanthanide(II)-Boron Complexes. Part II. Syntheses and Characterization of Cyanide-Bridged Lanthanide(III)-Palladium Complexes. Ph.D. Dissertation, The Ohio State University, Columbus, OH, 2001.

(20) Du, B.; Meyers, E. A.; Shore, S. G. Syntheses and Structural Characterizations of Sheet- and Column-like Lanthanide-Transition Metal Arrays: The Effect of Hydrogen Bonding on the Structure when K$^+$ is Replaced by [NH$_4$]$^+$. *Inorg. Chem.* **2001**, *40*, 4353–4360.

(21) Liu, J.; Meyers, E. A.; Shore, S. G. An Unusual Cyanide Bridging Lanthanide-Transition Metal Complex that Contains the One-Dimensional Cationic Array {[(DMF)$_{16}$Yb$_6$(μ_6-O)(μ_3-OH)$_8$(μ-NC)Pd-(μ-CN)(CN)$_2$]$^{6+}$}$_∞$. *Inorg. Chem.* **1998**, *37*, 5410–5411.

(22) Liu, S.; Meyers, E. A.; Shore, S. G. An Inclusion Complex with [Gd(DMF)$_8$]$^{3+}$ Ions Encapsulated in Pockets of an Anionic Array of {[Cu$_6$(CN)$_9$]$^{3-}$}$_∞$; A Cyanide-Bridged Cu–Gd Layer Structure. *Angew. Chem., Int. Ed.* **2002**, *41*, 3609–3611.